Uptake and Reaction of $ClONO_2$ on NaCl and Synthetic Sea Salt

Michael E. Gebel[†] and Barbara J. Finlayson-Pitts*

Department of Chemistry, University of California, Irvine, California 92697-2025

Received: December 31, 2000; In Final Form: March 15, 2001

The uptake and reaction of chlorine nitrate ($ClONO_2$) on NaCl and synthetic sea salt (SSS) powders was studied at 298 K using a Knudsen cell interfaced to a quadrupole mass spectrometer. A time-dependent uptake coefficient was observed, with a large initial uptake coefficient measured for most samples of $\gamma_{init} > 0.1$, followed by a smaller and slowly declining uptake coefficient at longer reaction times. This behavior is shown to be consistent with uptake into, and reaction in, water on the salt surface. The steady-state uptake coefficient on NaCl was invariant over a range of $ClONO_2$ concentrations from 10^{12} to 10^{13} molecules cm^{-3} but was dependent on the number of salt particle layers in a manner consistent with approximately two layers of particles being available for reaction. The results of experiments using monolayers and sub-monolayers of salts, where the available reactive surface is known, give an uptake coefficient at longer times after the rapid initial uptake for $ClONO_2$ on NaCl of $\gamma_t = (6.5 \pm 3.0) \times 10^{-3}$ (2σ). The larger uptake coefficient obtained initially compared to longer reaction times helps to reconcile different values reported earlier by other research groups for this reaction. The uptake coefficient on SSS, which holds more water, is much larger than that for NaCl, with $\gamma_{init} = (0.42^{+0.46}_{-0.42})$ and $\gamma_t = (0.16^{+0.20}_{-0.16})$ (2σ). At the higher uptake coefficients measured for SSS, this reaction could be a significant source of Cl_2 in the marine boundary layer if chlorine nitrate is available at a constant concentration of ∼5 ppt.

Introduction

The uptake and reaction of gases with sea salt aerosol can lead to the formation of gaseous inorganic chlorine compounds, including Cl_2, HCl, BrCl, $ClNO_2$, and $ClONO_2$. Some of these compounds can be photolyzed, producing chlorine atoms. Such a source of highly reactive atomic chlorine in the troposphere has the potential to impact the oxidative balance and overall air chemistry.[1−10] Chlorine atoms in the troposphere can react with either organics

$$Cl + RH \rightarrow HCl + R \quad (1)$$

or ozone:

$$Cl + O_3 \rightarrow ClO + O_2 \quad (2)$$

One possible subsequent reaction of the ClO formed in reaction 2 is reaction with NO_2 to form chlorine nitrate:

$$ClO + NO_2 \xrightarrow{M} ClONO_2 \quad (3)$$

Potential fates of $ClONO_2$ in the troposphere include deposition as well as hydrolysis on surfaces to form HOCl and nitric acid:

$$ClONO_2 + H_2O \rightarrow HOCl + HNO_3 \quad (4)$$

Further reaction of chlorine nitrate with the components of sea salt such as NaCl is also possible:[11−14]

$$ClONO_2 + NaCl \rightarrow Cl_2 + NaNO_3 \quad (5)$$

Subsequent photolysis of Cl_2 generates two chlorine atoms so that another chloride ion, in addition to the one from which $ClONO_2$ was formed, is activated. Clearly, understanding the kinetics of reaction 5 is important for assessing the role of chlorine chemistry in the marine boundary layer.

The kinetics of the reaction of chlorine nitrate with NaCl powders has been studied by two groups, with results differing by ∼2 orders of magnitude. Using a flow reactor, Timonen et al.[12] measured uptake coefficients in the range of 0.009−0.07; however, after correction for the effects of diffusion[15,16] into the salt layers, which accounts for the increased available surface area beyond the top surface geometric area, the final value reported was $(4.6 \pm 3.0) \times 10^{-3}$ at 296 K. Rossi and co-workers[13,14] used a Knudsen cell to study this reaction and reported the uptake coefficients to be 0.23 ± 0.06 and 0.10 ± 0.05, respectively. Similar kinetics were observed using thin, spray-deposited films of salt as well as bulk powder samples with multiple grain layers; as a result, they chose not to apply a correction for pore diffusion to their measured uptake coefficients. In all studies, Cl_2 was observed as the major reaction product in 100% yield, within experimental error.

We report here experimental studies of the uptake of $ClONO_2$ on powders of NaCl as well as on synthetic sea salt (SSS). We show that a large initial uptake, followed by smaller, long-term uptake, is consistent with water on the surface playing a major role in the uptake and reaction of $ClONO_2$. By using sub-monolayers of particles with well-defined sizes in some experiments, the role of diffusion into the multiple particle layers was probed and its impact on measurements made using multiple

* Author to whom correspondence should be addressed [telephone (949) 824-7670; fax (949) 824-3168; e-mail bjfinlay@uci.edu].

[†] Present address: Monitoring and Laboratory Division, California Air Resources Board, 9480 Telstar Ave., Ste. 4, El Monte, CA 91731.

10.1021/jp0046290 CCC: $20.00
Published on Web 05/05/2001

layers assessed. The results of the previous studies[12−14] are all shown to be consistent with our observations. The atmospheric implications are discussed.

Experimental Section

Experiments were performed in a glass Knudsen cell, described in detail elsewhere,[17] which is equipped with a movable lid for covering the sample. Reactant gases were introduced into the cell from a glass gas-handling manifold through a stainless steel needle valve coated with halocarbon wax (Halocarbon Products, series 1500). Salt powders, contained in one of two shallow, cylindrical Teflon holders with diameters of 3.1 and 4.9 cm, respectively, were placed on the sample platform prior to system pump-down. The Knudsen cell was interfaced to a quadrupole mass spectrometer (ABB Extrel, 150-QC) through one of two removable glass apertures with hole diameters of 3.9 and 5.8 mm, respectively.

Ion current signals were obtained by phase sensitive detection and processed with a lock-in amplifier (EG&G, model 5209) interfaced to a PC with data acquisition software (ABB Extrel, Merlin, rev. B). The species monitored by their parent ions included Cl_2 (*m*/*z* 70, 72, and 74), HOCl (*m*/*z* 52 and 54), HCl (*m*/*z* 36 and 38), and H_2O (*m*/*z* 18). In most cases, the parent ion with the most abundant isotopic composition was monitored after the species was identified by confirming the expected signal ratios. Chlorine nitrate was monitored by its fragments NO_2^+ (*m*/*z* 46), ClO^+ (*m*/*z* 51), and NO^+ (*m*/*z* 30). Uptake measurements were based on the NO_2^+ fragment (*m*/*z* 46) because it had the highest intensity and consequently the highest signal-to-noise ratio.

In the Knudsen cell, reactant gas molecules exit through an aperture into the mass spectrometer or are lost by uptake on the reactive surface. A net uptake coefficient, γ_{net}, can be determined from the ratio of the loss through the exit aperture to the loss on the surface. In our experiments, the measured uptake coefficient was derived from the relationship

$$\gamma_{net} = \frac{(I_0 - I_r)}{I_r}\left(\frac{A_{hole}}{A_{surf}}\right) \qquad \text{(I)}$$

Here, I_0 is equal to the steady-state reactant signal at the mass spectrometer with the surface covered, and I_r is equal to the reactant signal when the reactive surface is exposed. A_{hole} is the area of the exit aperture, and A_{surf} is the area of the reactive surface. In the initial data analysis, γ_{net} was calculated using the geometric surface area of the sample holder for A_{surf}; however, as discussed in detail below, the true reactive surface area was taken into account in the calculation of the final reaction probabilities.

The salts in these studies were obtained commercially: NaCl (Bicron, single crystals; or Fluka, powder), and synthetic sea salt (Aquarium Systems, Instant Ocean). Salts were prepared to yield two average grain sizes, fine and coarse. Coarse NaCl powders were generated by sieving commercially obtained powders or large single crystals (cuttings) that were ground by mortar and pestle. The fraction that passed through a no. 20 sieve but was retained by a no. 40 sieve was designated coarse. On the basis of the sieve sizes, these crystals should have average diameters between 425 and 850 μm;[18] however, they were examined using an optical microscope and found to be monodisperse cubic particles with average sides of 400 μm (Figure 1). SSS was sieved in the same manner to obtain particles of similar size. One experiment was performed using coarse NaCl that had been initially retained by the no. 40 sieve

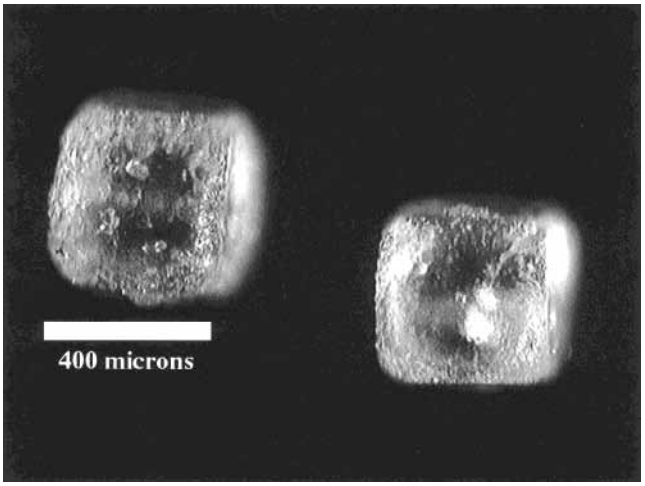

Figure 1. Image of coarse NaCl crystals at 120× magnification. (Figure is reproduced here at 50% of its original size.)

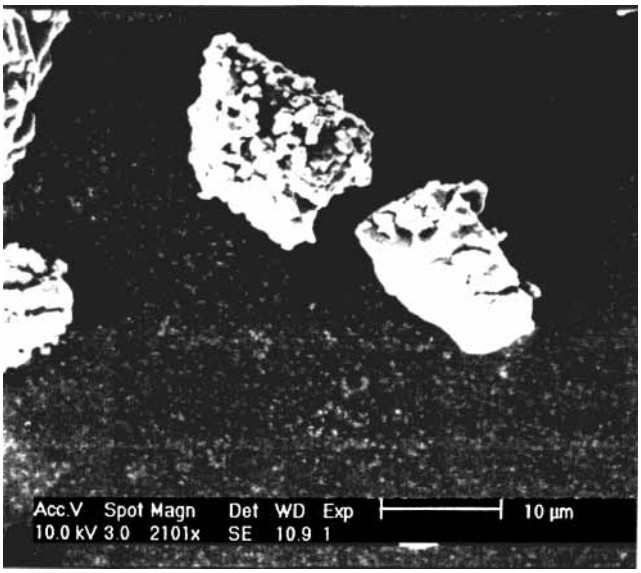

Figure 2. SEM image of fine NaCl crystals.

but passed through it with vigorous agitation; that is, these particles were just below the size that the no. 40 sieve could retain. Optical microscopy showed that these particles were cubic with sides of 300 μm on average. These samples were designated subcoarse.

Fine salts were those that resulted either from extensive grinding by mortar and pestle or by mechanical grinding in a Wig-L-Bug amalgamator (Crescent Dental, model 3110-3A) for 5 min. In an investigation of the reaction of NO_2 with NaCl and SSS ground using the Wig-L-Bug, Langer et al.[19] determined that fine NaCl powders had grain sizes between 1 and 10 μm and had a surface area of 2.9×10^3 cm^2/250 mg pellet. Assuming this powder consists of monodisperse nonporous cubes, each grain will have sides of 2.4 μm. They also showed that SSS powders generated by the Wig-L-Bug had grain sizes between 0.1 and 5 μm and a surface area of 2.4×10^4 cm^2/250 mg pellet. Again, assuming monodisperse, nonporous cubes, the sides will be 0.3 μm.

The NaCl finely ground by hand was shown by SEM to have a roughly bimodal distribution of average diameters of ~10 and <1 μm. Figure 2 shows an SEM image of this fine NaCl. On the basis of an estimate that there are <100 small particles for every 10 μm particle, the surface area of the large particles will

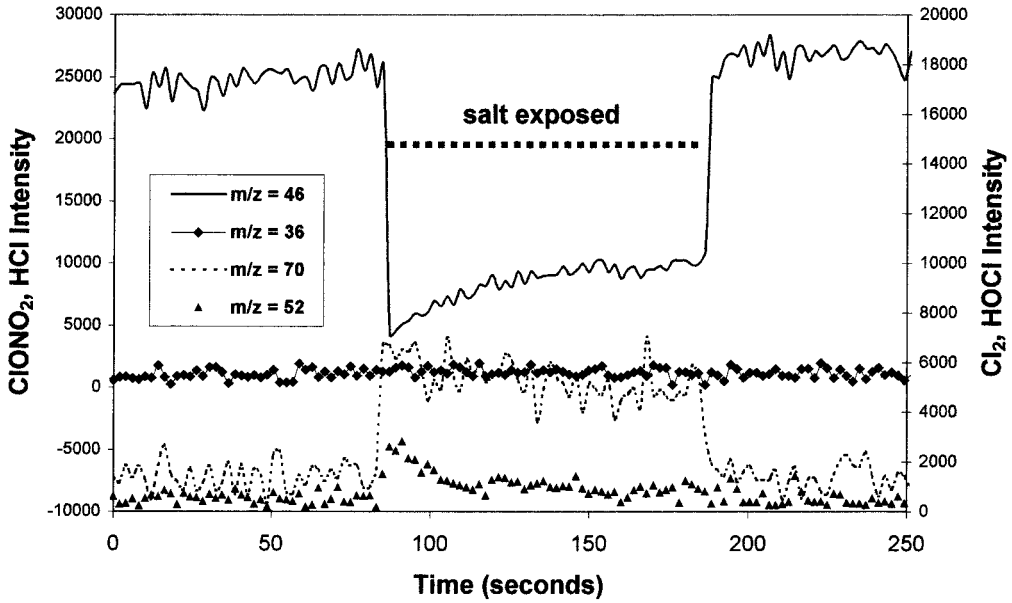

Figure 3. Uptake at 298 K of $ClONO_2$ (left axis) on 0.28 g (31 layers) of undried, unheated, fine NaCl and production of Cl_2 (right axis) and HOCl (right axis). The initial $ClONO_2$ concentration was 5.9×10^{12} molecules cm^{-3}. The signal at *m*/*e* 36 (left axis) is shown to demonstrate that there was no significant production of HCl. The diameter of the sample holder is 3.1 cm, and the aperture diameter is 5.8 mm.

account for >90% of the total surface area of the particles, and therefore fine salts were designated as having average diameters of 10 μm.

The number of salt layers for a given amount of salt in the sample holder was calculated as $(m/\rho_b Ah)$, where m is the mass (g) of the salt sample, ρ_b is the bulk density, A is the geometric area of the sample holder, and h is the height of one salt particle. The bulk density is the density of the unpacked powder in the sample holder. It was calculated from the measured mass that filled the known volume of the sample holder. For NaCl, $\rho_b =$ 1.2 g cm^{-3} for both grain sizes, and for SSS, $\rho_b = 1.2$ g cm^{-3} for fine particles and $\rho_b = 1.0$ g cm^{-3} for coarse particles. The difference in the bulk densities for fine compared to coarse SSS is due to the tendency of coarse SSS to form clumps that do not stack as efficiently. After grinding, salts were either immediately placed in the Knudsen cell or dried in an oven (100 °C) overnight. These dried salts, however, were exposed to ambient air for the short length of time required to weigh a sample and place it within the Knudsen cell, during which time water can be taken up from room air. The salts were pumped on while uncovered in the Knudsen cell prior to reaction. Some salt samples were heated during this pump down time by maintaining the sample platform temperature at 75° C in order to reduce the amount of water adsorbed to the powder.

$ClONO_2$ was synthesized by the reaction of HNO_3 with ClF (giving $ClONO_2$ and HF) using a method similar to that described by Schack.[20] Dry nitric acid was condensed in a glass trap by successive freezing of the vapor over a mixture of concentrated sulfuric and nitric acids (2:1 by volume). The trap was held at −115 °C using an ethanol bath and exposed to a molar equivalent of ClF. The mixture was allowed to warm to −70 °C for a few minutes to maximize the extent of reaction. Then the trap was brought back down to −115 °C, and any volatile byproducts were pumped off. Distillation of the $ClONO_2$ was performed by holding the reaction trap at −85 °C and the collection trap at −105 °C and gently pumping from the reaction trap into the collection trap. Brownish yellow chlorine nitrate liquid condensed in the collection trap over a period of minutes. At least 50% yield of $ClONO_2$ could be collected without any significant HF impurity condensed in the collection trap. Small amounts of HF could be removed by warming the trap to room temperature and allowing the HF to react with the glass, forming SiF_4 that could be pumped off of the collection trap after it was recooled to −115 °C.

Concentrated nitric acid (Fisher, 69.7 wt %) and sulfuric acid (Fisher, 96.0 wt %), Cl_2 (Matheson, high purity, 99.5%), HCl gas (Scott Specialty Gases, 99.995%), and ClF (Ozark-Mahoning Co.) were obtained commercially.

Results

$ClONO_2$ Reaction with NaCl Powders. Figure 3 shows the loss of chlorine nitrate and the production of Cl_2 in a typical experiment using fine NaCl powder that had not been dried or heated prior to exposure. A time-dependent uptake behavior is clearly seen, particularly during the first ~50 s. This uptake behavior is similar to that observed in previous studies with this system using HNO_3 or SO_2 as the reactant,[17,21,22] which was interpreted as due to initial uptake into water on the salt. Following the high initial uptake is a period of relatively stable, slowly declining, uptake.

Molecular chlorine was the major gaseous product observed; as seen in Figure 3, its production was anticorrelated with the loss of the reactant $ClONO_2$. Small amounts of HOCl, indicated by the signal at *m*/*z* 52, were produced initially but declined toward zero when the uptake of $ClONO_2$ appeared to reach a steady-state value. There was no evidence of production of gaseous HCl.

In several experiments, salts were heated for ~2 h while in the Knudsen cell before reaction. The loss of $ClONO_2$ and release of Cl_2 are shown for one of these experiments using dried, coarse, heated NaCl in Figure 4. The signal at *m*/*z* 52 due to HOCl was very small throughout the experiment, and there was no significant HCl production. For these samples, the difference between the initial uptake and the subsequent uptake was much less severe than for the finer, unheated salts.

As shown in Table 1, the average yield of Cl_2, $\Delta[Cl_2]/\Delta[ClONO_2]$, was measured in five experiments to be 81 ± 21% (2σ). The reported error is based on the calibrations for Cl_2 and $ClONO_2$ and is dominated by the relative error in $\Delta[ClONO_2]$.

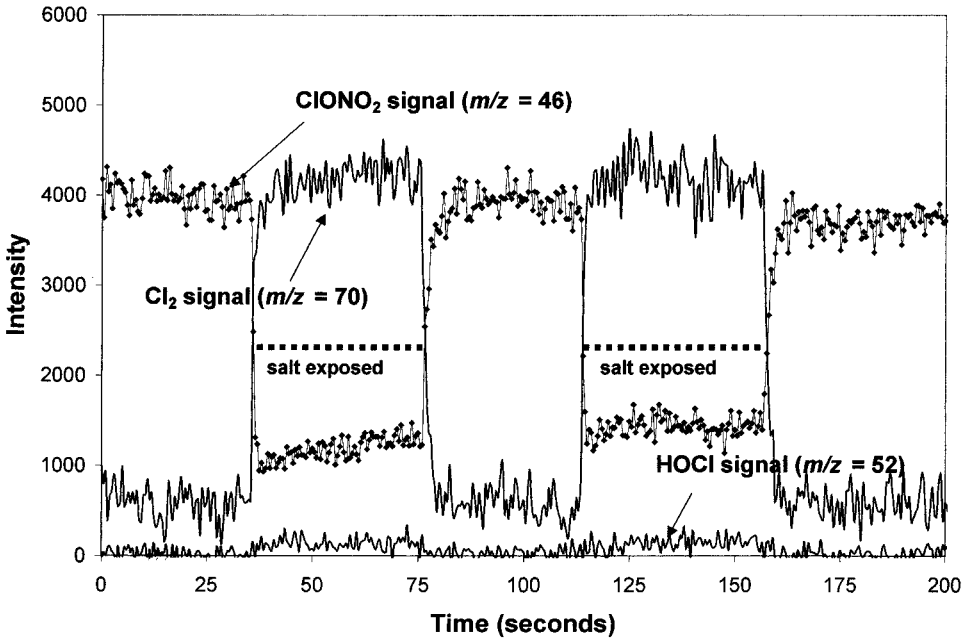

Figure 4. Uptake of $ClONO_2$ on 3.1 g (9 layers) of dried, coarse, heated NaCl. The initial $ClONO_2$ concentration was 4.6×10^{12} molecules cm^{-3}. The aperture is 3.9 mm, and the diameter of sample holder is 3.1 cm.

TABLE 1: Summary of Uptake Experiments and Generation of Cl_2 for $ClONO_2$ on NaCl

expt	size and pretreatment of salt[a]	av particle size[b] (μm)	total mass (g)	sample holder area (cm^2)	no. of particle layers[c]	aperture diameter (mm)	initial [$ClONO_2$] (molecules cm^{-3})	measured γ_{init}	measured γ_t	Cl_2 yield (%) ($\pm 2\sigma$)
1	fine	10	0.843	7.54	93	3.9		0.11	0.035	
2a	fine	10	1.425	7.54	158	3.9	1.4×10^{13}	0.13	0.056	
2b	fine	10	1.426	7.54	158	3.9	3.2×10^{13}	*f*	0.025	
3	fine	10	0.394	7.54	44	3.9	1.4×10^{13}	0.15	0.049	
4	fine	10	0.907	7.54	100	3.9	1.1×10^{13}	0.15	0.042	
5	fine	10	1.341	7.54	148	5.8	5.5×10^{12}	0.10	0.050	86 ± 68
6	fine	10	0.281	7.54	31	5.8	5.9×10^{12}	0.18	0.050	78 ± 40
7	coarse, dried	400	2.913	7.54	8	3.9	2.9×10^{12}	0.07	0.030	
8	coarse, dried	400	7.657	18.9	8	3.9	3.3×10^{12}	0.17	0.038	93 ± 23
9	fine	10	7.614	18.9	336	5.8	1.2×10^{13}	0.14	0.049	
10	fine	10	5.062	18.9	223	5.8	3.3×10^{12}	0.26	0.039	
11	fine	10	9.359	18.9	413	5.8	1.3×10^{13}	*h*	0.038	
12	coarse	400	1.413	7.54	3.9	3.9	1.1×10^{13}	0.06	0.035	
13	coarse, dried	400	1.338	7.54	3.7	5.8	8.8×10^{12}	>0.07	0.031	
14	coarse, dried, heated	400	3.257	18.9	3.6	3.9	2.3×10^{12}	*h*	0.033	83 ± 30
15	coarse, dried, heated	400	3.133	7.54	8.7	3.9	4.6×10^{12}	*h*	0.029	65 ± 57
16	fine, dried, heated	10	0.788	7.54	87	3.9	8.2×10^{12}	*h*	0.043	
17	fine, heated	10	2.982	7.54	329	3.9	2.4×10^{13}	*h*	0.033	
							average[i] ($\pm 2\sigma$):	0.14 ± 0.11	0.039 ± 0.018	81 ± 21
18	subcoarse	300	0.211	7.54	0.8	5.8	6.5×10^{11}	0.13	0.019	
19	coarse	400	0.101	7.54	0.3	5.8	2.0×10^{12}	0.24	0.0072	
20	coarse	400	0.0895	7.54	0.2	5.8	1.3×10^{12}	0.02	0.0063	
21	coarse	400	0.0594	7.54	0.2	5.8	1.6×10^{12}	0.007	0.0024	
22	large crystals[g]	2500	2.650	7.54	1.2	5.8	5.9×10^{12}	0.17	0.021	
23	fine	10	0.921	7.54	102	1.3	3.9×10^{13}	*d*	≥ 0.020[e]	

[a] See text for a description of the method of preparation of each type of sample. [b] Crystal size was determined by microscopy (see text). [c] Determined using the bulk density and average crystal height; see text for method of calculation. [d] I_r was reduced to baseline level making measurement of γ_{init} impossible. [e] Represents a lower limit to γ. [f] This salt was previously exposed to $ClONO_2$. [g] These crystals were large enough to measure by hand with calipers. [h] The initial uptake for these samples showed little enhancement relative to the longer term uptake. [i] Average ($\pm 2\sigma$) for γ_{init} was calculated for multilayer experiments with measured values only.

The small amounts of HOCl produced were not quantified, but from the weak signals (Figures 3 and 4) and high yields of Cl_2, HOCl clearly must be a minor product.

The uptake of $ClONO_2$ was measured using samples of various sizes, numbers of salt layers in the sample holder, and methods of sample treatment (e.g., heating and pumping). Although most experiments were carried out with multilayer samples, five involved the use of less than a monolayer of crystals, the size of which had been measured using optical microscopy or, in one case, manually using calipers. The results for multi- versus sub-monolayer coverage of the sample holder are presented in the following sections; the implications for diffusion and reaction of $ClONO_2$ beyond the top layer of thick samples are treated in detail subsequently.

Effects of Multiple Salt Layers on Uptake. Table 1 shows the measured uptake coefficients calculated by assuming A_{surf}

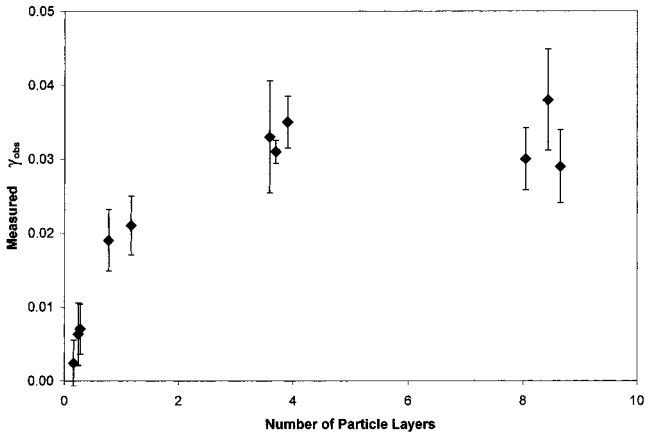

Figure 5. Measured γ_t as a function of the number of particle layers for coarse NaCl samples.

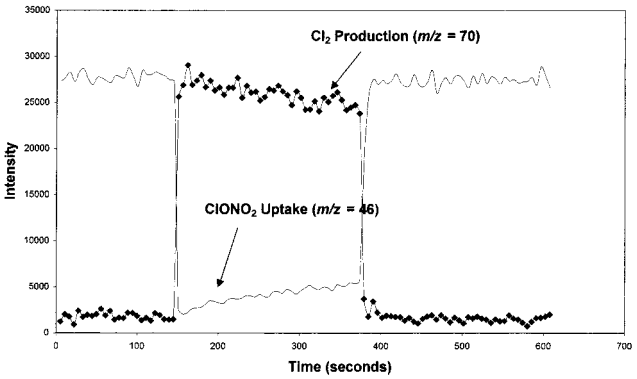

Figure 6. Uptake at 298 K of $ClONO_2$ on 0.39 g (43 layers) of dried but unheated, fine SSS, and production of Cl_2. The initial $ClONO_2$ concentration was 8.6×10^{12} molecules cm^{-3}. The diameter of the sample holder is 3.1 cm, and the aperture diameter is 5.8 mm.

is the geometric area of the sample holder. Two different values are given for most experiments: (1) that for the initial rapid uptake, γ_{init}, and (2) that at slightly longer times where the uptake coefficient is smaller and changes less rapidly, γ_t. Generally, for multiple layers of salts that are expected to hold significant amounts of water, for example, fine, unheated samples,[17,19,21] a high initial uptake is observed, with γ_{init} in the range of $\sim 0.1-0.3$. For these samples, γ_t falls in the range from 0.025 to 0.056. The value of γ_t fell slowly with time. For example, the measurement of $\gamma_t = 0.025$ for experiment 2b was performed on the salt sample used in experiment 2a ($\gamma_t = 0.056$) in which it had been repeatedly exposed to $ClONO_2$. With these multilayer samples, the value of γ_t was, within experimental error, independent of the number of layers of the salt.

Monolayer and Sub-monolayer Samples. Five experiments (18−22) were performed using coarse salt samples of mass and size calculated to give approximately a monolayer or less than a monolayer coverage of the salt on the sample holder. This was confirmed by visual inspection; the individual salt crystals could be seen to be distributed over the bottom of the sample holder. Because the particle size in these experiments had been well characterized, the total reactive surface area is known and diffusion into, and reaction with, additional layers of the sample is not relevant.

Because the available surface area is less than the geometric area of the sample holder used to calculate γ_t and γ_{init}, the measured values of the reaction probabilities are expected to be lower than for the multilayer experiments. The data in Table 1 show that this is indeed the case, with γ_t ranging from 0.002 to 0.02. Figure 5 shows the values of γ_t as a function of the number of particle layers for coarse NaCl samples, where the particle sizes and shapes are relatively uniform and well characterized. Whereas the measured uptake coefficient is invariant with the number of particle layers for more than two layers, it drops off at monolayer and sub-monolayer coverage.

$ClONO_2$ Uptake on Synthetic Sea Salt Powders. Figure 6 shows the loss of $ClONO_2$ and the production of Cl_2 for a typical experiment using SSS. The experiments performed on SSS are summarized in Table 2. The values of γ_{init} are again large, ranging from ~ 0.1 to 0.8, larger than those for NaCl.

Cl_2 was again the major gaseous reaction product observed. The yields of Cl_2 during the steady-state uptake were measured for three experiments and are shown in Table 2. The average is $78 \pm 13\%$ (2σ), which is within experimental error of the yield for the reaction with NaCl. The generation of small amounts of HCl and HOCl was observed in some experiments.

Unlike the experiments with NaCl, SSS samples would routinely degas quantities of water when the lid was uncovered sufficiently to measurably raise the total pressure to between 1 and 9 mTorr in the Knudsen cell during the first seconds of uptake. If released in an instantaneous burst, this would be equivalent to $\sim(0.2-2) \times 10^{17}$ molecules of water released from salt samples ranging from 0.3 to 2.1 g in mass; a direct correlation between sample mass and pressure increase cannot be made as the burst is more dependent on drying conditions.

Discussion

These experiments show that there are three regimes for reaction: (1) a rapid initial uptake and reaction which is controlled by water on the salt surface, (2) a smaller and slowly declining uptake into the water layer which occurs over longer periods of time after the initial rapid uptake, and (3) a slow passivation of the surface by reaction. Reaction to generate Cl_2 occurs in all regimes.

Rapid Initial Uptake. That the rapid initial uptake is controlled by water on the salt surface is indicated by three observations. First, this initial "spike" in the uptake is seen primarily with finely ground salts that have not been heated and pumped on prior to the reaction; such samples have been shown in previous studies to hold significant amounts of water, which control the reactivity.[17] Second, this high initial uptake is exacerbated in the case of reaction with SSS, which holds much larger amounts of water than NaCl.[19,21] Third, a spike in the production of gaseous HOCl is observed initially (Figure 3), as expected from the hydrolysis, reaction 4 above, of $ClONO_2$.

The reaction of gaseous HNO_3 with NaCl is known to generate gaseous HCl:[17,21,23−31]

$$HNO_3 + NaCl \rightarrow HCl + NaNO_3 \qquad (6)$$

In earlier studies of the reaction of gaseous HNO_3 with NaCl in this laboratory,[17] we interpreted the production of HCl as being due to the uptake of HNO_3 into water on the salt, causing the pH to fall until HCl degassed. Thus, the HNO_3 generated in the hydrolysis of $ClONO_2$ will first acidify the water layer. If sufficient acidification occurs, the generation of gas-phase HCl is expected.[17] However, as seen in Figure 3, in the present experiments no significant amounts of HCl were observed. This may reflect the fact that there is another mechanism besides degassing of HCl for consuming acid in this system, the acid-

TABLE 2: Summary of Uptake Experiments and Generation of Cl_2 for $ClONO_2$ on Synthetic Sea Salt (SSS)

expt	size and pretreatment of salt	av particle size[b] (μm)	total mass (g)	sample holder area (cm^2)	no. of particle layers[c]	aperture diameter (mm)	initial [$ClONO_2$] (molecules cm^{-3})	measured γ_{init}	measured γ_t	Cl_2 yield (%) ($\pm 2\sigma$)
24	fine	10	0.578	7.54	64	5.8	4.9×10^{12}	0.45	0.08	
25	fine	10	2.135	7.54	236	5.8	3.6×10^{12}	0.28	0.06	
26	coarse, dried	400	0.983	7.54	3.3	5.8	5.2×10^{12}	0.37	0.15	
27	coarse, dried	400	1.200	7.54	4.0	3.9	8.7×10^{12}	0.22	0.14	
28	coarse, dried	400	1.170	7.54	3.9	3.9	1.7×10^{13}	0.76	0.16	
29	coarse, heated	400	1.273	7.54	4.3	3.9		0.12	0.09	
30	coarse	400	1.048	7.54	3.5	3.9		0.11	0.05	
31	fine, dried	10	0.335	7.54	37	5.8	7.8×10^{12}	0.60	0.32	74 ± 11
32	fine, dried	10	0.388	7.54	43	5.8	8.7×10^{12}	0.44	0.16	74 ± 12
33	fine, dried	10	0.295	7.54	33	5.8	9.7×10^{12}	0.80	0.36	85 ± 15
							average ($\pm 2\sigma$):	0.42 ± 0.46	0.16 ± 0.20	78 ± 13

[a] See text for a description of the method of preparation of each type of sample. [b] Crystal size was determined by microscopy (see text). [c] Determined using the bulk density and average crystal height; see text for method of calculation.

catalyzed reaction of HOCl with chloride ions:[32]

$$HOCl + Cl^- + H^+ \rightarrow Cl_2 + H_2O \qquad (7)$$

Thus, HCl may be consumed in the secondary reaction 7, and the water layer may not become sufficiently acidic to expel HCl into the gas phase.

If the initial uptake of $ClONO_2$ on NaCl and SSS is due to uptake into, and reaction in, water on the salt surface, it may be described at least semiquantitatively in terms of a liquid resistance model often applied to the uptake of gases into liquids.[10,33,34] This behavior was observed previously using this system to study the uptake of SO_2 on SSS.[22] Given that we are dealing in the present case with small amounts of water on solid salts, rather than pure liquids, such an approach is semiquantitative at best. However, it supports interpretation of the rapid initial uptake as being due to uptake into a liquid-like surface. According to this model, if diffusion of the gas to the surface is fast, the net uptake coefficient is approximated by

$$\frac{1}{\gamma_{net}} = \frac{1}{\alpha} + \frac{1}{\Gamma_{sol} + \Gamma_{rxn}} \qquad (II)$$

Here, α is the mass accommodation coefficient and the solubility and reaction terms are given by eqs **III** and **IV,** respectively:

$$\Gamma_{sol} = \frac{4H^*RT}{\bar{c}}\sqrt{D_l/\pi t} \qquad (III)$$

$$\Gamma_{rxn} = \frac{4H^*RT}{\bar{c}}\sqrt{D_l k_{rxn}} \qquad (IV)$$

H^* is the effective Henry's law coefficient; R is the gas constant; T is the temperature; $\bar{c}$ is the mean speed of the gas (for $ClONO_2$ at 298 K, 2.5×10^4 cm s^{-1}); D_l is the liquid-phase diffusion coefficient (for $ClONO_2$ in water at 298 K, D_l is estimated[35] to be on the order of 1×10^{-5} cm^2 s^{-1}); and k_{rxn} (s^{-1}) is a pseudo-first-order reaction rate to account for reaction in the bulk aqueous phase, which affects the net uptake. The behavior of the $ClONO_2$ upon first exposing the salt ($t \rightarrow 0$) is controlled by physical transport across the gas−liquid interface, that is, $\gamma_{net}^{t\rightarrow 0} = \gamma_{init} \rightarrow \alpha$. The values of the uptake coefficient measured immediately after exposure, γ_{init}, for the multiple layers of salts that showed distinct time-dependent behavior are seen in Table 1 to be in the range from 0.06 to 0.26 for NaCl and in Table 2 to be in the range from 0.11 to 0.80 for SSS. The mass accommodation coefficient, α, for $ClONO_2$ on water does not appear to have been measured directly in other studies for comparison to this value; however, the recommended value[36] of the reaction probability for $ClONO_2$ on ice over the range 180−200 K is 0.3, similar to the initial uptake coefficient on water at room temperature measured here.

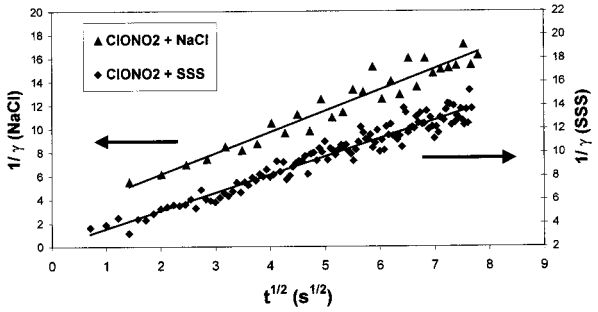

Figure 7. $1/\gamma_{obs}$ vs $t^{1/2}$ for undried, unheated, fine samples of NaCl (upper plot) and SSS (lower plot).

If the subsequent decrease in the uptake after the very high initial values is due to the surface water becoming saturated with $ClONO_2$, $1/\gamma$ should show a dependence on the square root of time. As seen in Figure 7, the time dependence of the uptake on NaCl and SSS samples that were not dried or heated does indeed follow a $t^{1/2}$ dependence in the initial stages of the reactions.

This effect of water on the uptake and reaction of $ClONO_2$ is not surprising, given similar effects on the reaction of HNO_3 with NaCl and sea salt. For example, Beichert and Finlayson-Pitts[17] described the reactive uptake of HNO_3 as effectively uptake into, and reaction in, an aqueous phase. De Haan and Finlayson-Pitts[21] reported even larger amounts of water on SSS powder and hence chemistry similar to that for NaCl. Allen et al.[29] showed that water exposure after the reaction of HNO_3 with NaCl could effectively reactivate the surface. Davies and Cox[26] reported that the uptake of HNO_3 increased with increasing water vapor pressure and proposed a surface mechanism involving water. Ghosal and Hemminger[30] subsequently showed their data and those of Davies and Cox are both[26] consistent with a water-induced mobilization of the $NaNO_3$ product on the surface.

In summary, the rapid initial uptake of $ClONO_2$ both on NaCl and on SSS is controlled by water on the surface of the salts. Both the production of HOCl from the reaction with undried NaCl during this initial uptake and the $t^{-1/2}$ dependence of γ_{init} are consistent with the role of water in this initial uptake. Note, however, that during the initial rapid uptake, Cl_2 is also being generated. Hence, although water is a controlling factor, a

TABLE 3: Summary of Experiments at Monolayer and Sub-monolayers of Salt

expt	particle size (μm)	total mass (g)	sample holder area (cm^2)	no. of particle layers	total surface area[a] A_{spec} (cm^2)	measured steady-state[b] γ_{obs}	corrected for true surface area[c] γ_{true}
18	300	0.2107	7.54	0.8	19.5	0.019	0.0074
19	400	0.1011	7.54	0.3	7.0	0.0072	0.0075
20	400	0.0895	7.54	0.2	6.2	0.0063	0.0077
21	400	0.0594	7.54	0.2	4.1	0.0024	0.0044
22	2500	2.6501	7.54	1.2	29.4	0.021	0.0054
						average ($\pm 2\sigma$):	0.0065 ± 0.0030

[a] Calculated assuming monodisperse cubic crystals (see text). [b] Measured as described in text using the geometric surface area, $A_{surf} = 7.54$ cm^2. [c] Calculated using A_{surf} = total surface area in column 6.

combination of dissolution and reaction of $ClONO_2$ must be occurring even in this initial stage.

Uptake at Longer Times. The slower and continuously declining uptake of $ClONO_2$ must also involve water on the surface. For example, the observation that the steady-state uptake can continue for several hundred seconds or more suggests that this uptake does not occur by a simple gas−solid interaction mechanism. If $ClONO_2$ reacted with a dry, solid NaCl surface, the surface would quickly become covered with the solid reaction product, $NaNO_3$. At 0.1 mTorr, $ClONO_2$ has a collision rate of 1.5×10^{17} s^{-1} with a 7.54 cm^2 NaCl geometric surface area. Assuming $\gamma = 0.005$,[12] the time required for a number of *reactive* collisions equal to the number of atoms on the surface, $\sim 5 \times 10^{15}$ surface chloride (based on 6.4×10^{14} Cl atoms cm^{-2}), is ~6 s. However, our experiments show the uptake occurs for more than several hundred seconds, even with much higher chlorine nitrate concentrations, without showing significant signs of surface deactivation. Clearly, the uptake of $ClONO_2$ on NaCl (and SSS) powders is not a simple gas−solid interaction. This is not surprising considering that there is water associated with the powders and that numerous previous studies have indicated that such water affects the uptake of other reactive gases on NaCl (and SSS) powder.[14,17,19,21,26−30,37−39]

If this reaction system was truly uptake of $ClONO_2$ into a bulk aqueous phase as described by eqs **II**−**IV**, the net observed uptake, γ_{net}, would approach a constant value. At this point, the solution would be saturated with $ClONO_2$ and its time-independent uptake would be due to removal in the liquid phase by reaction, eq **IV**. However, in the present studies γ_{net} was observed to slowly decline with time in the second regime following the rapid, initial uptake. This is not surprising given that there is no bulk aqueous phase but, rather, small amounts of water on some as yet unknown sites on the solid salt surfaces. The continuing slow decline of γ_{net} with time may be due to passivation of the salt surface as the reaction proceeds and forms nitrate on the surface. Thus, the analogy with uptake into bulk aqueous solutions represented by eqs **II**−**IV** is primarily useful in providing a semiquantitative approach to interpreting the initial rapid uptake when γ_{net} approaches α.

The measured values of the uptake coefficients are based on the assumption that only the geometric surface area of the sample is available for reaction, that is, that there is no significant diffusion of $ClONO_2$ into the salt when multiple layers are present. For both the fine and coarse NaCl with more than approximately four layers of salt, there is no significant dependence of the measured uptake coefficient on the number of layers (Figure 5), showing that the $ClONO_2$ does not probe the salt below these top four layers. However, whether it penetrates into the top two or three layers cannot be determined from these multilayer experiments.

The data obtained using coarse NaCl powders at coverages at and below a monolayer provide some insight into this question. Table 3 summarizes the data for the experiments at approximately a monolayer or less where the available surface area, A_{spec}, is well-defined. A_{spec} can be unambiguously determined for samples consisting of a single species with known particle size and geometry. Previous studies[12,19,37] have established that the salts are nonporous, that is, their BET surface area is effectively given by the surface area of the crystal faces, so the total surface area for these samples is $A_{spec} = 6d^2N$, where d is the length of a side and N is the total number of particles (assuming that the portion of the crystals making contact with the sample holder is also available for reaction). Values for γ_t calculated using the specific surface area of the sample, A_{spec}, are given in Table 3 as γ_{true}. It can be seen that values of the uptake coefficient for these experiments calculated using the known surface area are significantly smaller than the values measured in the experiments using multiple layers of salt, with an average corrected value of $(6.5 \pm 3.0) \times 10^{-3}$ (2σ). This suggests that although the measured, larger, average value of γ_t of 0.039 ± 0.018 for the multilayer experiments is invariant with the number of layers from 4 to 413, it must reflect the availability of more than the top layer of particles.

The packing of the salt into the sample holder leaves the top surface structure quite porous. Knowing the total volume of the sample holder when filled and the salt mass and solid density, the porosity of the surface can be calculated, that is, the fraction of the geometric surface area that is open. For 500 μm particles, the porosity is 0.35; that is, for every two salt particles on the surface, there is an opening equivalent in size to one salt particle. Given this porosity, it is reasonable to assume that all six sides of the crystals in the top layer are available for reaction, rather than just one as would be the case for a smooth surface of zero porosity.

To probe how many layers of salt are involved in the $ClONO_2$ reaction, we applied the model developed by Keyser, Moore, and Leu[15,16] (KML model). According to the KML model, the true uptake coefficient, γ_{true}, is related to the measured value, γ_{obs}, in the following manner

$$\gamma_{obs} = \gamma_{true}\left(\frac{A_e + \eta A_i}{A_{geo}}\right) \qquad \text{(VI)}$$

where A_e is the external surface area (i.e., top of the surface layer), A_i is the internal surface area of the sample, A_{geo} is the geometric surface area of the sample holder, and η is an effectiveness factor. The effectiveness factor is the fraction of the internal surface area that is available to the reactant gas that diffuses into the pores of the sample. That is, there is a finite depth of the sample that the reactant gas will be able to penetrate during exposure. A large effectiveness factor indicates that the gas can penetrate through many internal particle layers and thus be exposed to a higher effective surface area during the uptake period. In the limit of very slow reactions, the gas can probe

TABLE 4: Estimated Effectiveness Factors for Multilayer Experiments with NaCl

expt	size and pretreatment of NaCl	particle size (μm)	no. of particle layers	sample holder area (cm^2)	measured γ_t	effectiveness factor[a] η	no. of particle layers probed by $ClONO_2$
1	fine	10	93	7.54	0.035	0.007	1.6
2a	fine	10	157	7.54	0.056	0.01	2.6
2b	fine	10	157	7.54	0.025	0.001	1.2
3	fine	10	44	7.54	0.049	0.030	2.3
4	fine	10	100	7.54	0.042	0.010	2.0
5	fine	10	148	7.54	0.050	0.009	2.3
6	fine	10	31	7.54	0.050	0.044	2.4
7	coarse, dried	400	8	7.54	0.030	0.056	1.5
8	coarse, dried	400	8	18.9	0.038	0.103	1.9
9	fine	10	336	18.9	0.049	0.004	2.3
10	fine	10	223	18.9	0.039	0.004	1.8
11	fine	10	413	18.9	0.038	0.002	1.8
12	coarse	400	3.9	7.54	0.035	0.216	1.8
13	coarse, dried	400	3.7	7.54	0.031	0.163	1.6
14	coarse, dried, heated	400	3.6	18.9	0.033	0.206	1.7
15	coarse, dried, heated	400	8.7	7.54	0.029	0.045	1.4
16	fine, dried, heated	10	87	7.54	0.043	0.012	2.0
17	fine, heated	10	329	7.54	0.033	0.002	1.5
						average:	1.9 ± 0.8

[a] Calculated using eq VII and $\gamma_{true} = 6.5 \times 10^{-3}$ from the monolayer and sub-monolayer experiments.

all of the salt sample surface and the BET surface area of the salt is the appropriate reactive area. A small effectiveness factor reflects the fact that the reaction is sufficiently fast that the gas reacts at the surface before being able to penetrate into the salt. As $\eta \rightarrow 0$ and $A_e \rightarrow A_{geo}$, then $\gamma_{obs} \rightarrow \gamma_{true.}$ When $\gamma_{obs} > 0.1$, corrections to the measured uptake coefficient for increased available surface area beyond the geometric area are usually ignored.[15]

Equation **VI** is equivalent[16,40] to

$$\gamma_{obs} = \gamma_{true}\rho_b S_{BET}(h_e + \eta h_i) \qquad \text{(VII)}$$

where ρ_b is the bulk density, S_{BET} is the BET specific surface area ($cm^2\ g^{-1}$), h_e is the height of the first layer, and h_i is the height of all the internal layers. The effective number of layers probed by $ClONO_2$ in the multilayer experiments can be estimated using $\gamma_{true} = (6.5 \pm 3.0) \times 10^{-3}$ from the sub-monolayer experiments. Knowing the particle size, the height of particles in the top layer (h_e) and of the internal layers (h_i), the bulk density (ρ_b) and the BET surface area S_{BET}, the effectiveness factor, η, can be calculated from the measured values of γ_{obs}. In previous studies, the salts were shown by BET measurements to be nonporous,[12,19,37] and hence the geometric surface area of the crystals is also their BET surface area. Thus, S_{BET} can be calculated from the measured dimensions of the cubic crystals and the true density of the salt. Table 4 shows the values of the effectiveness factor calculated in this manner. The number of particle layers probed will be equal to one (the top layer) plus this effectiveness factor times the total number of internal layers. On average, about two layers of NaCl react with $ClONO_2$.

Comparison with Previous Studies. Leu and co-workers[12] used a flow tube holding salt samples on the bottom and followed the loss of $ClONO_2$ and formation of Cl_2 with time. The measured values of the uptake coefficient were in the range of 0.009−0.07, which is similar in magnitude to the values measured here using multiple salt layers. They argue that the effective reactive surface area of the salt is larger than the top geometric area due to the fact that diffusion and reaction of $ClONO_2$ in the subsurface layers can occur. To correct for this, they applied their previously developed KML model[15,16] to correct their measured values of the uptake coefficients to obtain the final reported value of $(4.6 \pm 3.0) \times 10^{-3}$ (2σ). Our value based on the monolayer and sub-monolayer experiments in which the available reactive surface areas are reasonably well-known, $\gamma_{true} = (6.5 \pm 3.0) \times 10^{-3}$ (2σ), is within experimental error of their value corrected for surface area.

Rossi and co-workers[13,14] used a Knudsen cell similar to that in the present studies and reported values for the uptake coefficient of 0.23 ± 0.06 and 0.10 ± 0.05, respectively, in reasonably good agreement with each other. They did not correct for diffusion into lower layers of the salt because the measured uptake coefficients were independent of the nature of the salt sample, that is, ground powders and grains as well as single crystals and thin films where diffusion into lower layers is not possible. They measured these values using two different experimental methods. In the steady-state approach, the uptake coefficients were determined from the drop in the reactant signal when the plunger covering the salt sample was lifted. In a second approach, a pulse of gas was introduced into the cell and its decay followed with time, out to ~2 s; this was done both with the salt covered and with it exposed to the gas. The exponential decays of $ClONO_2$ were fit to obtain the additional uptake due to reaction with the salt when it was exposed. In these pulsed valve experiments where the fit is over approximately the first second of the reaction, the uptake would likely reflect predominantly the initial uptake which in our experiments is larger than the steady-state values (Table 1). The values they obtained in the pulsed experiments were in excellent agreement with those from the steady-state approach, which occur over much longer periods of time. However, if the steady-state values were calculated on the basis of the first opening of the lid, these would also correspond to our values of γ_{init}. Our measured values for γ_{init} for the multilayer salt experiments ranged from 0.06 to 0.26, with an average of 0.14 ± 0.11 (2σ), in excellent agreement with the measurements of Rossi and co-workers.[13,14]

Both sets of previous studies also reported that Cl_2 was formed in 100% yield, within experimental error. Timonen et al.[12] reported HOCl formation when high water vapor (3×10^{-3} Torr) concentrations were present during the reaction. Aguzzi and Rossi[14] did not observe HOCl production in the reaction with NaCl, but did when $ClONO_2$ hydrolyzed on nonreactive salt surfaces such as Na_2SO_4. These results are in agreement

with the results presented here, where only small signals due to HOCl were observed in some experiments at short reaction times.

In short, the results presented here are in good agreement with both sets of previous determinations of the uptake coefficient for $ClONO_2$ on NaCl if the two different reaction regimes are separated; that is, there is a rapid initial uptake represented by γ_{init} , followed by a slower uptake represented by γ_t. In addition, there is agreement that Cl_2 is the major gaseous product.

Determination of γ for $ClONO_2$ on Synthetic Sea Salt. The uptake coefficients for $ClONO_2$ on SSS were almost always >0.1. Keyser, Moore, and Leu[15] show that under these conditions of rapid uptake, diffusion into the salt is not important because the gas reacts before it can diffuse into lower layers. Under these conditions, the correction to the measured values of the uptake coefficients is less than a factor of 3, which is on the order of the scatter in the data (Table 2). In addition, any such correction would be highly uncertain due to the heterogeneous chemical composition of individual salt crystals. We have therefore not corrected our measured values of the uptake coefficients for the reaction of $ClONO_2$ with SSS for diffusion into the salt.

The average values we measured here were $\gamma_{init} = 0.42 \pm 0.46$ and $\gamma_t = 0.16 \pm 0.20$, where the errors are the 2σ statistical errors. Because a negative value of the uptake coefficient is not physically possible, the lower error bounds must be adjusted, giving $\gamma_{init} = (0.42^{+0.46}_{-0.42})$ and $\gamma_t = (0.16^{+0.20}_{-0.16})$. Thus, the uptake both initially and at longer reaction times is high and variable. This is not surprising, given the large amounts of water associated with SSS and the inhomogeneity of the crystal composition. For example, Langer et al.[19] and Weis and Ewing[38] have shown that sea salt particles contain pockets of water in microcrystalline and amorphous regions in addition to water from crystalline hydrates such as $MgCl_2 \cdot 6H_2O$.

Reaction Mechanism. On the basis of the evidence that water is strongly affecting the uptake of $ClONO_2$ on both NaCl and SSS, the mechanism of reaction is likely to be similar to that proposed by Beichert and Finlayson-Pitts[17] for the uptake and reaction of HNO_3 with NaCl. Thus, the $ClONO_2$ is first taken up into water on the surface and then reacts within a concentrated solution on the salt particle. The mechanism is expected to be similar for NaCl and SSS, with the possible exception of the presence of buffers such as $CaCO_3$ in the case of SSS.

The reaction of $ClONO_2$ with HCl on ice at low temperatures (probably in a quasi-liquid layer on the ice surface) is well-known with respect to polar stratospheric cloud chemistry:[10,36,41−44]

$$ClONO_2 + HCl \xrightarrow{ice} Cl_2 + HNO_3 \qquad (6)$$

The reaction is believed to involve an ionic mechanism, with attack of the Cl^- formed from dissociation of HCl on the $ClONO_2$.[10,41−46] Reaction 6 may also occur via the initial formation of HOCl formed by hydrolysis of $ClONO_2$

$$ClONO_2 + H_2O \rightarrow HOCl + HNO_3 \qquad (4)$$

followed by the well-known acid-catalyzed reaction of HOCl with the chloride ion:[32]

$$HOCl + Cl^- + H^+ \rightarrow Cl_2 + H_2O \qquad (7)$$

The chemistries of $ClONO_2$ on both NaCl and SSS holding water at room temperature are similar. The production of HOCl initially in some experiments is consistent with its hydrolysis (reaction 4). However, this reaction simultaneously produces nitric acid, which acidifies the water. As a result, reaction 7 becomes more important, and the generation of HOCl in the gas phase falls with time, as was observed. No induction time was observed for the production of Cl_2 within the limits of our experiments. We cannot distinguish whether a direct reaction of $ClONO_2$ also occurs with chloride ions to generate Cl_2 or whether HOCl is an essential intermediate in the production of Cl_2 by reaction 4 followed by reaction 7. However, the fact that HCl is a very minor product shows that the water layer does not become sufficiently acidic to degas significant amounts of HCl, as occurs in the direct HNO_3−NaCl reaction.[17,23−27,30] This suggests that there is a reaction or reactions that lead to acid consumption, which is the case for reaction 7.

Atmospheric Implications. Using $\gamma = 6.5 \times 10^{-3}$, the amount of Cl_2 generated by this reaction for a typical sea salt aerosol concentration of 1 cm^{-3} can be estimated if we assume 2.5 μm cubic NaCl particles and a background $ClONO_2$ concentration of 5 ppt.[4,47] Under these conditions, 2×10^3 molecules of Cl_2 are generated per second. This would lead to a concentration of 3.5 ppt of Cl_2 after 12 h of darkness. This estimate assumes a source of $ClONO_2$ that maintains a steady-state concentration of 5 ppt despite the consumption of approximately that amount in one night and that the steady-state kinetics characteristic of "dry" NaCl is the appropriate value to use.

However, in the marine boundary layer, the relative humidity is generally above the deliquescence point and, hence, the use of the larger value of the initial uptake coefficient for sea salt may be more appropriate. Using $\gamma_{init} = 0.42$ measured using SSS, the rate of production of Cl_2 could be as high as 1.3×10^6 molecules cm^{-3} s^{-1}, which would generate ~200 ppt of Cl_2 in 12 h. This is clearly an overestimate because it again assumes a constant concentration of $ClONO_2$ and does not take into account the possible production of HOCl. However, it is noteworthy that this is of the same order of magnitude as measurements of Cl_2 in the marine boundary layer by Spicer and co-workers,[48] which peaked at ~150 ppt, and of non-HCl inorganic chlorine compounds by Keene, Pszenny, and co-workers.[49,50]

Conclusions

The uptake coefficient for $ClONO_2$ on NaCl powder is initially large (>0.1) due to the effect of water adsorbed to the surfaces of the powder. These results are consistent with the high uptake observed by Rossi and co-workers[13,14] measured during initial exposure of the salt. The initial uptake follows a $t^{-1/2}$ dependence under "wet" conditions, as would be expected due to the effect of solubility on the uptake of $ClONO_2$ into the water associated with the powders. The uptake of $ClONO_2$ on SSS follows a similar time dependence but is even greater than that on NaCl due to the effect of higher surface water, with $\gamma_{init} = (0.42^{+0.46}_{-0.42})$.

At longer reaction times, there is a smaller uptake coefficient for $ClONO_2$ on NaCl powders with a measured value of 0.039 ± 0.018 (2σ). Whereas this value does not depend on the number of layers of salt particles over the range from 4 to 413, experiments at monolayer and sub-monolayer coverages show that approximately two particle layers react and that the true steady-state uptake coefficient is $(6.5 \pm 3.0) \times 10^{-3}$ (2σ). This is consistent with the value of $(4.3 \pm 3.0) \times 10^{-3}$ reported by Leu and co-workers.[12]

The yield of Cl_2 was measured to be close to unity for both the NaCl and SSS reactions. In most cases, small amounts of

HOCl were observed, particularly at short reaction times, suggesting that hydrolysis of $ClONO_2$ also occurs. It may be that the mechanism of these reactions involves hydrolysis of $ClONO_2$ to generate HOCl, followed by the well-known acid-catalyzed reaction with chloride ions to generate Cl_2.

With these reaction probabilities, this reaction may be a significant contributor to the observed[48−50] levels of Cl_2 at night in the marine boundary layer.

Acknowledgment. We thank the National Science Foundation and the Department of Energy for support of this research. We also thank M. Zach and R. M. Penner for valuable microscopy assistance, J. C. Hemminger, M.-T. Leu, M. J. Rossi and J. N. Pitts, Jr., for helpful discussions, and M. Rossi and V. Grassian for providing preprints prior to publication.

References and Notes

(1) Keene, W. C.; Pszenny, A. A. P.; Jacob, D. J.; Duce, R. A.; Galloway, J. N.; Schultz-Tokos, J. J.; Sievering, H.; Boatman, J. F. *Global Biogeochem. Cycles* **1990**, *4*, 407.

(2) Finlayson-Pitts, B. J. *Res. Chem. Intermed.* **1993**, *19*, 235.

(3) Keene, W. C. Inorganic Cl Cycling in the Marine Boundary Layer: A Review. In *Naturally-Produced Organohalogens*; Grimvall, A., Leer, E. W. B. D., Eds.; Kluwer Academic Publishers: Dordrecht, The Netherlands, 1995; p 363.

(4) Sander, R.; Crutzen, P. J. *J. Geophys. Res.* **1996**, *101*, 9121.

(5) Vogt, R.; Crutzen, P. J.; Sander, R. *Nature* **1996**, *383*, 327.

(6) Finlayson-Pitts, B. J.; J. N. Pitts, J. *Science* **1997**, *276*, 1045.

(7) Ravishankara, A. R. *Science* **1997**, *276*, 1058.

(8) Andreae, M. O.; Crutzen, P. J. *Science* **1997**, *276*, 1052.

(9) DeHaan, D. O.; Brauers, T.; Oums, K.; Stutz, J.; Nordmeyer, T.; Finlayson-Pitts, B. J. *Int. Rev. Phys. Chem.* **1999**, *18*, 343.

(10) Finlayson-Pitts, B. J.; Pitts, J. *Chemistry of the Upper and Lower Atmosphere—Theory, Experiments, and Applications*; Academic Press: San Diego, CA, 2000.

(11) Finlayson-Pitts, B. J.; Ezell, M. J.; Pitts, J. *Nature* **1989**, *337*, 241.

(12) Timonen, R. S.; Chu, L. T.; Leu, M.-T.; Keyser, L. F. *J. Phys. Chem.* **1994**, *98*, 9509.

(13) Caloz, F.; Fenter, F. F.; Rossi, M. J. *J. Phys. Chem.* **1996**, *100*, 7494.

(14) Aguzzi, A.; Rossi, M. J. *Phys. Chem. Chem. Phys.* **1999**, *1*, 4337.

(15) Keyser, L. F.; Moore, S. B.; Leu, M.-T. *J. Phys. Chem.* **1991**, *95*, 5496.

(16) Keyser, K. F.; Leu, M.-T.; Moore, S. B. *J. Phys. Chem.* **1993**, *97*, 2800.

(17) Beichert, P.; Finlayson-Pitts, B. J. *J. Phys. Chem.* **1996**, *100*, 15218.

(18) Lide, D. R. *Handbook of Chemistry and Physics*, 74th ed.; CRC Press: Boca Raton, FL, 1994.

(19) Langer, S.; Pemberton, R. S.; Finlayson-Pitts, B. J. *J. Phys. Chem. A* **1997**, *101*, 1277.

(20) Schack, C. J. *Inorg. Chem.* **1967**, *6*, 1938.

(21) DeHaan, D. O.; Finlayson-Pitts, B. J. *J. Phys. Chem. A* **1997**, *101*, 9993.

(22) Gebel, M. E.; Finlayson-Pitts, B. J.; Ganske, J. S. *Geophys. Res. Lett.* **2000**, *27*, 887.

(23) Fenter, F. F.; Caloz, F.; Rossi, M. J. *J. Phys. Chem.* **1994**, *98*, 9801.

(24) Leu, M.-T.; Timonen, R. S.; Keyser, L. F.; Yung, Y. L. *J. Phys. Chem.* **1995**, *99*, 13203.

(25) Fenter, F. F.; Caloz, F.; Rossi, M. J. *J. Phys. Chem.* **1996**, *100*, 1008.

(26) Davies, J. A.; Cox, R. A. *J. Phys. Chem. A* **1998**, *102*, 7631.

(27) Laux, J. M.; Hemminger, J. C.; Finlayson-Pitts, B. J. *Geophys. Res. Lett.* **1994**, *21*, 1623.

(28) Laux, J. M.; Fister, T. F.; Finlayson-Pitts, B. J.; Hemminger, J. C. *J. Phys. Chem.* **1996**, *100*, 19891.

(29) Allen, H. C.; Laux, J. M.; Vogt, R.; Finlayson-Pitts, B. J.; Hemminger, J. C. *J. Phys. Chem.* **1996**, *100*, 6371.

(30) Ghosal, S.; Hemminger, J. C. *J. Phys. Chem. A* **1999**, *103*, 4777.

(31) Hemminger, J. C. *Int. Rev. Phys. Chem.* **1999**, *18*, 387.

(32) Wang, T. X.; Margerum, D. W. *Inorg. Chem.* **1994**, *33*, 1050.

(33) Kolb, C. E.; Worsnop, D. R.; Zahniser, M. S.; Davidovits, P.; Keyser, L. F.; Leu, M.-T.; Molina, M. J.; Hanson, D. R.; Ravishankara, A. R.; Williams, L. R.; Tolbert, M. A. Laboratory Studies of Atmospheric Heterogeneous Chemistry. In *Progress and Problems in Atmospheric Chemistry*; Barker, J. R., Ed.; World Scientific: Singapore, 1995; Vol. 3; Chapter 18.

(34) Kolb, C. E.; Jayne, J. T.; Worsnop, D. R.; Davidovits, P. *Pure Appl. Chem.* **1997**, *69*, 959.

(35) Houghton, G. *J. Chem. Phys.* **1964**, *40*, 1628.

(36) DeMore, W. B.; Sander, S. P.; Golden, D. M.; Hampson, R. F.; Kurylo, M. J.; Howard, C. J.; Ravishankara, A. R.; Kolb, C. E.; Molina, M. J. Chemical Kinetics and Photochemical Data for Use in Stratospheric Modeling, Evaluation No. 12; JPL Publication 97-4, NASA Jet Propulsion Laboratory: Pasadena, CA, January 15, 1997.

(37) Vogt, R.; Finlayson-Pitts, B. J. *J. Phys. Chem.* **1994**, *98*, 3747.

(38) Weis, D. D.; Ewing, G. E. *J. Phys. Chem. A* **1999**, *103*, 4865.

(39) Weis, D. D.; Ewing, G. E. *J. Geophys. Res.* **1999**, *104*, 21.

(40) Underwood, G. M.; Li, P.; Usher, C. R.; Grassian, V. H. *J. Phys. Chem. A* **1999**, *104*, 819.

(41) Molina, M. J.; Tso, T.-L.; Molina, L. T.; Wang, F. C.-Y. *Science* **1987**, *238*, 1253.

(42) Tolbert, M. A.; Rossi, M. J.; Malhotra, R.; Golden, D. M. *Science* **1987**, *238*, 1258.

(43) Tolbert, M. A.; Rossi, M. J.; Golden, D. M. *Geophys. Res. Lett.* **1988**, *15*, 847.

(44) Leu, M.-T. *Geophys. Res. Lett.* **1988**, *15*, 17.

(45) Gilligan, J. J.; Castleman, A. W., Jr. *J. Phys. Chem. A* **2001**, *105*, 1028.

(46) Oppliger, R.; Allanic, A.; Rossi, M. J. *J. Phys. Chem. A* **1997**, *101*, 1903.

(47) Singh, H. B.; Kasting, J. F. *J. Atmos. Chem.* **1988**, *7*, 261.

(48) Spicer, C. W.; Chapman, E. G.; Finlayson-Pitts, B. J.; Plastridge, R. A.; Hubbe, J. M.; Fast, J. D.; Berkowitz, C. M. *Nature* **1998**, *394*, 353.

(49) Keene, W. C.; Maben, J. R.; Pszenny, A. A. P.; Galloway, J. N. *Environ. Sci. Technol.* **1993**, *27*, 866.

(50) Pszenny, A. A. P.; Keene, W. C.; Jacob, D. J.; Fan, S.; Maben, J. R.; Zetwo, M. P.; Springer-Young, M.; Galloway, J. N. *Geophys. Res. Lett.* **1993**, *20*, 699.